ELSEVIER

Advances in Water Resources 25 (2002) 1069–1089

Advances in Water Resources

www.elsevier.com/locate/advwatres

Detailed physics, predictive capabilities and macroscopic consequences for pore-network models of multiphase flow

Martin J. Blunt *, Matthew D. Jackson, Mohammad Piri, Per H. Valvatne

Department of Earth Science and Engineering, Imperial College, Prince Consort Road, London SW7 2BP, UK

Received 29 September 2001; received in revised form 14 January 2002; accepted 27 May 2002

Abstract

Pore-network models have been used to describe a wide range of properties from capillary pressure characteristics to interfacial area and mass transfer coefficients. The void space of a rock or soil is described as a network of pores connected by throats. The pores and throats are assigned some idealized geometry and rules are developed to determine the multiphase fluid configurations and transport in these elements. The rules are combined in the network to compute effective transport properties on a mesoscopic scale some tens of pores across. This approach is illustrated by describing a pore-scale model for two- and three-phase flow in media of arbitrary wettability. The appropriate pore-scale physics combined with a geologically representative description of the pore space gives a model that can predict average behavior, such as capillary pressure and relative permeability. This capability is demonstrated by successfully predicting primary drainage and waterflood relative permeabilities for Berea sandstone. The implications of this predictive power for improved characterization of subsurface simulation models are discussed. A simple example field study of waterflooding an oil-wet system near the oil/water contact shows how the assignment of physically-based multiphase flow properties based on pore-scale modeling gives significantly different predictions of oil recovery than using current empirical relative permeability models. Methods to incorporate pore-scale results directly into field-scale simulation are described. In principle, the same approach could be used to describe any type of process for which the behavior is understood at the pore scale.

Keywords: Multiphase flow in porous media; Pore-scale modeling; Network models

1. Introduction

In network modeling rules are developed that describe the pertinent physical processes and arrangements of fluid within each pore. These rules are then combined to describe flow and transport in systems approximately tens of pores across, representing samples of around 1 mm to a few cm cubed. From this macroscopic properties of the behavior can be computed. A common example of this approach is to use pore-scale modeling to predict relative permeability and capillary pressure as a function of average saturation. This approach was pioneered by Fatt in the 1950s [1–3]. Refs. [4,5] give excellent historical reviews of pore-network modeling, while [6] provides a recent bibliography. Other excellent papers that comprehensively describe this approach include [7–10]. Local capillary equilibrium and the Young–Laplace equation are used to determine multiphase fluid configurations for any pressure difference between phases for pores of different shape and with different fluid/solid contact angles. The pressure in one of the phases is allowed to increase and a succession of equilibrium fluid configurations are computed in the network. Then empirical expressions for the hydraulic conductance of each phase in each pore and throat are used to define the flow of each phase in terms of pressure differences between pores. Conservation of mass is invoked to find the pressure throughout the network, assuming that all the fluid interfaces are frozen in place. From this the relationship between flow rate and pressure gradient can be found and hence macroscopic properties, such as absolute and relative permeabilities, can be determined.

* Corresponding author. Tel: +44-20-7594-6500; fax: +44-20-7594-7444.

E-mail address: m.blunt@ic.ac.uk (M.J. Blunt).

0309-1708/02/$ - see front matter
PII: S0309-1708(02)00049-0

In principle, any type of process that can be described at the pore scale can be incorporated in a network model to compute effective properties at a larger scale. In recent years there has been an explosion of interest in pore-scale modeling with studies of a huge range of phenomena, such as mass transfer, interfacial area, dispersion, electrical properties and foam flow [11–28].

Conceptually this approach to understanding flow and transport in porous media is distinct from other methods. The relevant transport equations are not solved directly in the pore space. Examples of such approaches are Stokes solutions for flow in single pores with specified geometry [29], or lattice Boltzmann methods [30,31]. These techniques provide a more rigorous description of different physical processes, but are often limited to relatively simple physical situations, or to systems encompassing only a few pores. However, they provide effective parameters at the pore scale to be used in network modeling. In network modeling, macroscopic equations, such as Darcy's law, are not invoked directly, but emerge from averaging the relevant pore-scale physics. For this reason, pore-scale modeling is quite different from larger-scale traditional simulation approaches for transport in porous media, where the macroscopic constitutive relationships are assumed a priori.

In this paper we will not attempt to review the vast and growing literature on pore-scale modeling, but will focus on a few outstanding issues of interest to the authors. In Section 2 we will describe what has become recently the standard model for describing two-phase flow in media of different wettability following the work of Øren, Patzek and co-workers [10,32,33]. Since these papers provide a clear and comprehensive discussion of all the mathematical details, we will not repeat them here. Instead we will provide a more conceptual discussion that emphasizes the key steps. We will start with a brief review of methods to describe the pore space (Section 2.1) before outlining two-phase pore-scale displacement mechanisms for drainage and waterflooding (Sections 2.2–2.6). Section 2.7 will show some example results to demonstrate that pore-network models can predict multiphase flow properties in a geologically representative model of the pore space. In Section 3 we will briefly describe how this model can be extended to study three-phase flow (water, oil, and gas or air) and some example results will be presented (Section 3.2). Section 4 deals with pore-network modeling of different physical processes: dispersion, dissolution and electrical properties. Section 5 discusses how the quasi-static models described so far can be extended to study rate-dependent effects. In Section 6 the implications of having predictive models are discussed in terms of improved characterization and simulation of multiphase flow processes.

2. Two-phase quasi-static network modeling

2.1. Description of the pore space

Most networks are based on a regular lattice—typically a cubic lattice with a coordination number of six. It is possible to vary the coordination number by eliminating throats from the network [34–37]. The network can be distorted by allowing the throat lengths to vary [38]. With an arbitrary distribution of throat lengths the resultant network may not even be physically realizable in three dimensions. However, in all these cases the network is still based on a regular topology, whereas the porous medium it is attempting to model has a more irregular structure. To overcome this limitation studies have been made using networks based on square or cubic lattices but with extra coordination [7], Voronoi networks [38–40], Delaunay triangulations [39,40] and irregular networks that allow a variable coordination number [41].

Another approach is to construct a random network where the connectivity is based on a representation of a real porous medium. First it is necessary to obtain a three-dimensional representation of the pore space. This is normally a pixellated image of pore and grain at some appropriate resolution. Fig. 1a shows an image of the pore space of a sandstone obtained from a geological reconstruction (see below for details of how this is done). Then a network of pores and throats is constructed, with properties such as shape and volume assigned to each element in the network that mimics the three-dimensional image. Finding a topologically equivalent skeleton to describe the network is non-trivial, but has been achieved by several authors [10,33,42–46]. A schematic of such a network is shown in Fig. 1b.

There are several ways in which a three-dimensional description of the pore space, as shown in Fig. 1, is obtained. The pore structure can be constructed directly. A series of two-dimensional sections can be combined to form a three-dimensional image [47,48]. However, this process is laborious. Another approach is to use X-ray microtomography to image the three-dimensional pore space directly at resolutions of around a micron [49–52]. This method is direct and accurate to the resolution of the machine, but to date is not a routine method for core analysis. Two-dimensional thin sections are, in contrast, often readily available. The porosity and two-point correlation function can be measured from these sections and used to generate a three-dimensional image with the same statistical properties. This has the advantage of being quite general, allowing a wide variety of porous media to be described [43,44,46,53–61]. In most of these studies, an equivalent network is not actually constructed—instead flow simulations are performed directly on the image of the pore space. For instance, Adler et al. modeled Fontainebleu sandstone

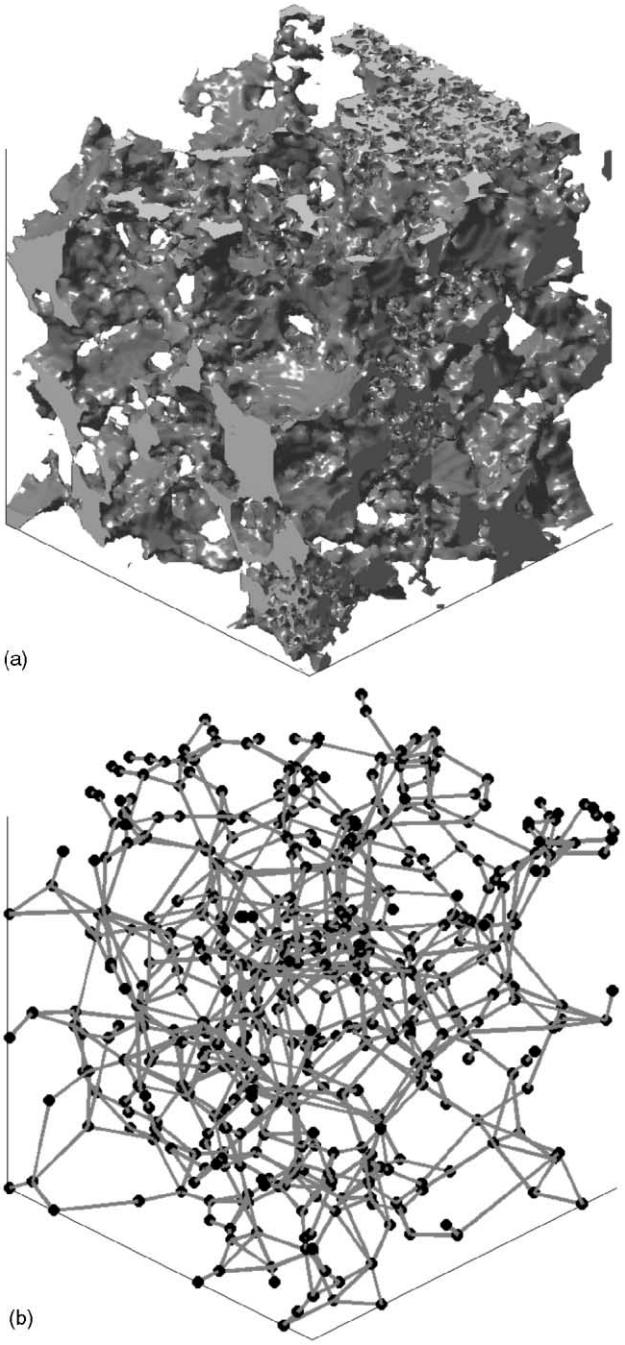

Fig. 1. Representations of the pore space of sandstone samples from Øren et al. [10,32]. (a) A three-dimensional image of the pore space at a resolution of 3 μm. The image was produced by simulating the geological processes—sedimentation of spherical grains of different size, followed by compaction, diagenesis and the addition of clays—by which the sandstone was formed. (b) A topologically equivalent network of pores connected by throats. The pores and throats are assigned volumes, conductances, inscribed radii and shapes that mimic essential features of the reconstructed pore space.

using a statistical technique to generate a three-dimensional pore space that had the same porosity and two-point correlation function as thin section images. He successfully predicted absolute permeability and electrical properties [62,63]. As we discuss below, the disadvantage is that the simulated pore space may ignore the long-range connectivity of the pore space imposed by the geological processes that formed it [32,64]. This is because it is difficult to impose this connectivity through matching two-point statistics alone. This leads to an alternative approach—reconstruction of the porous medium by modeling the geological processes by which it was made.

Bryant and co-workers pioneered the use of geologically realistic networks [65–68]. They based their models on a random close packing of equally-sized spheres. They represented diagenesis by swelling the spheres uniformly and allowing them to overlap. They modeled compaction by moving the centers of the spheres closer together in the vertical direction, again allowing the spheres to overlap. Equivalent networks with a coordination number of four or less were then constructed. Single and multiphase flow was simulated through the pore space. They were able to predict the absolute and relative permeability, capillary pressure, and electrical and elastic properties of water-wet sand packs, sphere packs and a cemented quartz sandstone, and to predict the trend of permeability with porosity for Fontainebleu sandstone. This represented a major triumph in pore-scale modeling, since genuine predictions of transport and flow properties were made for the first time. They showed that spatial correlations in the pore size distribution were important for correct predictions: using the same pore size distribution, but assigning it at random to the throats in the network gave erroneous predictions of permeability [65]. The major problem with the work was its restricted application—it could only be applied to media that were, to a good approximation, composed of spherical grains of the same size.

The next major advance came with the work of Øren, Bakke and co-workers at Statoil [10,32,42,64,69]. They developed a reconstruction method, where the packing of spheres of different size was simulated. The grain size distribution was derived directly from analysis of thin sections of the rock of interest. Compaction and diagenesis was modeled in a similar manner to Bryant et al. Clays were also included in the model. Biswal et al. [64] compared the pore space derived from this geological reconstruction of a Fontainebleau sandstone with an image obtained from microtomography. They also studied two stochastic models based on a correlation function representation. They showed that the stochastic models differed strongly from the real sandstone in their connectivity properties. The geological reconstruction gave a good representation of the connectivity of the rock and as a consequence could accurately predict transport properties [32].

Øren et al. [10,42] used the geological reconstructions to construct topologically equivalent networks through which multiphase flow was simulated. The same

approach to pore-space description and multiphase flow will be followed in this paper and described in the sections that follow. They predicted relative permeability for a variety of water-wet sandstones, showed promising results for a mixed-wet reservoir sample [32] and matched three-phase water-wet data [69].

This work offers the exciting possibility of predictive modeling for a variety of realistic systems. Pillotti [45] and Coehlo et al. [70] have shown how to simulate the deposition of grains of non-spherical shapes, enabling, in principle, the reconstruction technique to be applied more generally. Other authors have also predicted single and multiphase properties using sphere packs [33,54,71].

There are three major concerns with the application of reconstruction methods to reservoir samples, however. First, the reconstruction algorithm is based on explicit simulation of the geological processes by which the rock is formed. For many complex systems, involving microporosity and clays and a variety of different sedimentary processes, this may prove challenging. Furthermore, carbonate systems are not modeled at all. Statistical reconstruction methods are more general, since they require only a two-dimensional image of the system, and have been applied successfully to non-clastic rocks [59]. However, so far, their application has been principally to predict single-phase flow simulated directly on the pore-space reconstruction. In principle though this work could be extended to study multiphase flow properties using an equivalent network representation of the pore space. The second problem, for any approach, is that characterization of the pore space requires detailed thin section analysis that might not be available or difficult to obtain. Third, the appropriate characterization of pore shape and wettability is not completely understood. These issues will be discussed in more detail below.

The conclusion of this brief review is that a description of the pore space with a disordered connectivity based on the real system of interest is sufficient to produce a predictive model in some circumstances. Network models based on a regular lattice can always be tuned to match particular experimental results of interest. Indeed, there is a large body of work using different empirical methods to adjust network model parameters to experimental data (see, for instance [34–37,72]). This provides some assurance that pore-scale models do represent flow and transport properties adequately, but the matching process is generally non-unique. This means that there is no guarantee that the geometry of the pore space is close to the real system, and as a consequence there is little confidence that the model could be used to predict other properties reliably. Instead, an approach that represents the real geometry and topology of the pore space is needed to make genuine predictions.

2.2. Pore shape and wetting layers

The shapes assigned to pores and throats are also significant in defining transport properties. Most early work in pore-scale modeling assumed that the throats were cylinders with a circular cross-section. Pores were either not modeled explicitly at all (they simply connected throats together), or were spherical or cylindrical in shape. The assumption of an effective circular cross-section is reasonable for predicting single-phase properties, or the relative permeability of the non-wetting phase that resides in the centers of the larger pore spaces. For instance, for the sphere packs studied by Bryant et al. [65,66], the true cross-section of the throats was a grain boundary shape formed by the intersection of three or four spheres. They defined an effective radius that was the arithmetic mean of the inscribed radius and a radius of a circle with the same cross-sectional area as the throat. This effective radius varied along the throat. To account for this in a computation of permeability, they found the hydraulic conductance of each throat from an analytical calculation of the flow through a series of frustra (truncated cones). For multiphase flow, the capillary entry pressure for the non-wetting phase depended on the minimum effective radius along the throat. For saturation computations, the volume of the throat was computed directly from the pore structure. No explicit computation for pores was made. So conceptually, the network was composed of throats of circular cross-section connected at pores with no volume. However, the volumes, hydraulic conductance and capillary entry pressures of the throats were carefully calculated based on the description of the real pore space. This is the 'three R's' approach used by the Heriot–Watt group [34–36]—they too considered a lattice of cylindrical throats with no volume assigned to pores. However, they used independent expressions for the capillary entry pressure, the volume of a throat and the hydraulic conductance. This is equivalent to using different values of the radius R in the expressions for capillary pressure, volume and conductance. In this way, in principle, a rather general network model can be constructed with the parameters determined from a three-dimensional image of the pore space or tuned to match available experimental data. To recap, there are three different 'sizes' that are important: an inscribed radius to determine the capillary pressure at which a non-wetting fluid will enter the element; a radius that controls the volume; and a hydraulic radius than controls fluid conductance. When representing real porous media these quantities are not necessarily simply related.

In multiphase flow, when the non-wetting phase occupies the center of a pore or throat, the wetting phase may reside in grooves, crevices of roughness in the pore space. These wetting layers have been observed directly in micromodel experiments [73]. Wetting layers are sta-

bilized by capillary forces and have a typical thickness of a few microns—comparable to, although smaller than—the size of the pores. Flow through these layers, although slow, is measurable and can have a significant effect on the displacement. This is in contrast to wetting films that are stabilized by molecular forces and are typically nanometers thick. Flow though such films is negligible. In a sphere pack with smooth grains, the wetting phase can form pendular rings of fluid around the grain contacts. The wetting phase may apparently reside in layers, but the pendular rings are not connected and the wetting phase can be trapped. This was observed in bead packs by Dullien et al. [74] where a trapped wetting phase saturation of approximately 10% was found. They then roughened the beads by etching them in acid—the beads then contained micron-scale roughness as observed from SEM images. When a fully water-saturated pack was drained in air, water (wetting) phase saturations as low as 1% were reached. This implies that in porous media composed of rough grains the wetting layers are connected and provide a conduit for flow, albeit slow, down to low saturation. The consideration of wetting layers in pore-scale modeling studies is essential to reproduce even the qualitative behavior of electrical properties, three-phase flow, relative permeability hysteresis, dissolution rate and unsaturated flow in fractures [10–18,44,69,75–87]. In these cases, having pores with only single-phase occupancy, or disconnected wetting phase, allowed insufficient connectivity of the wetting phase and resulted in poor comparisons with experiment. At very low wetting phase saturation, adsorbed water films, nanometers in thickness, in addition to wetting layers, have a significant impact on capillary pressure [85,86].

It is difficult to represent every nook and cranny in the pore space directly. A simpler approach, adopted by many authors, is to assign some simple shape to the pore and throat cross-sections that accommodates wetting layers. Just as in the assignment of effective pore sizes, there is no suggestion that the real pore space is represented by some idealized constant cross-section—the shape is chosen simply to place the correct volume of wetting phase in layers in a pore whose center is filled by non-wetting phase and to give the right hydraulic conductivity to the layers. A variety of different shapes have been proposed, including fractal models of roughness [14,15,44], grain boundary pore shapes [11–14,75], squares [17,38,76,77] and triangles [10,78]. Øren et al. [10] defined a shape factor, G, for each pore and throat. The shape factor is the ratio of the cross-sectional area to the perimeter length squared. They then modeled the element as having a circular, square or scalene triangular cross-section such that the shape of the cross-section had the same shape factor as the reconstructed pore space they were modeling. In most cases the pores and throats had a triangular cross-section, as shown in Fig. 2.

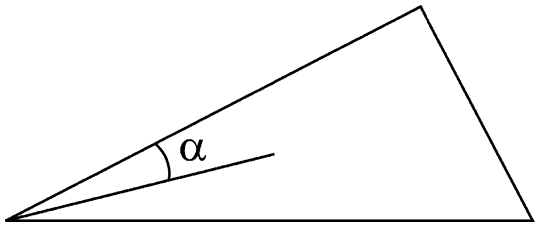

Fig. 2. The irregular cross-section of a pore or throat is represented by a scalene triangle with the same shape factor (ratio of cross-sectional area to perimeter squared) as the relevant section of the three-dimensional image of the porous medium. The inscribed radius and volume of the element are also obtained from the pore space reconstruction. The configuration of fluids in the element is determined by its wettability and the half angle α of the corners.

The details of how this was done are explained in [10, 33]. When non-wetting phase occupies the pore centers, wetting phase can reside in the corners. The volume of wetting phase in the corners depends on the capillary pressure. It is further assumed that all the wetting layers are connected to those in adjacent pores and throats.

For multiphase flow consideration of wetting layers is essential to model correctly the behavior of the wetting phase. It is not known at present if the characterization of pores as having triangular cross-sections is sufficiently detailed to capture this flow accurately.

2.3. Changes in wettability

Few, if any, hydrocarbon reservoirs are strongly water-wet and many soils contaminated by oil often display oil-wet characteristics. The reason for this is that the prolonged contact of oil with the solid surface allows surface-active components of the oil to adhere to the solid surface, changing its wettability [88]. For strongly water-wet media the different displacement mechanisms for multiphase flow are well established from micromodel studies [73] and have been used in pore-scale models to explain a variety of phenomena, including relative permeability hysteresis, and trends in residual oil saturation [8,89]. For media of arbitrary wettability, there is less direct experimental evidence of the appropriate pore-scale arrangements of fluid and their macroscopic consequences. However, below we outline a simple and appealing theoretical pore level scenario for wettability alternation that appears to capture the pertinent physics of non-water-wet displacements.

Kovscek et al. [90] proposed a pore-level model of wettability change and fluid distribution. Consider a displacement sequence that mimics oil migration and production in a hydrocarbon reservoir. Initially we consider the reservoir rock to be completely saturated with water and to be water-wet. During oil migration, oil invades the pore space. Where the oil directly contacts the solid its wettability changes. Regions of the

pore space for which a thick wetting film of water coats the surface remain water-wet, as do the corners of the pore space where water still resides, and pores that remain completely water-filled. The degree of wettability alteration depends on the composition of the oil and water, the mineralogy of the solid surface and the capillary pressure imposed during primary drainage [88,90]. In laboratory studies, wettability alteration typically takes 40 days to complete [88]. This is a shorter time than oil resides in reservoirs before being produced, or even typical residence times for oil in polluted aquifers. Then oil is displaced from the pore space by flooding with water. During this process we assume that the wettability does not change. Kovscek et al. examined the pore-scale configurations of fluid and the macroscopic behavior for a bundle of parallel tubes with a grain boundary shape [90]. Within a single pore, the surfaces have different wettability, as shown in Fig. 3 for a triangular pore. This results in a number of different possible fluid configurations during waterflooding. If portions of the pore wall are oil-wet, then water reenters the pore-space as the non-wetting phase and occupies the centers of the pore-space. Oil may reside as a layer sandwiched by water in the corner and water in the center (Fig. 3(b)). This provides connectivity of the oil and allows for very low residual oil saturations to be reached. Using this pore-level scenario the effects of waterflood relative permeability on wettability have been explored in detail using network modeling [35, 36,77]. Dixit et al. introduced the regime theory that explained hitherto puzzling experimental trends in recovery in terms of wettability characterized by a contact angle for the oil-wet regions and the fraction of pores that become oil-wet [35,91].

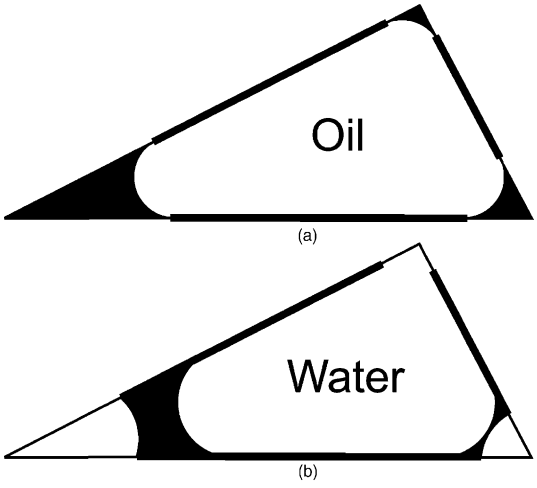

Fig. 3. Oil and water in a triangular pore or throat. (a) After primary drainage, oil fills the center of the pore space while water remains in the corners. The areas directly contacted by oil (shown by the bold line) have an altered wettability, while the corners that are water-filled remain water-wet. (b) If the surfaces of altered wettability are strongly oil-wet, then during water injection, the water fills the center of the pore. Water also remains in the corners, leaving a layer of oil sandwiched in between.

2.4. Two-phase drainage

We refer the reader to a number of excellent papers on this topic [8,10,33] for the mathematical details of how a network model simulates multiphase displacement. However, we will describe the conceptual basis of pore-scale modeling and discuss the approximations made.

We will follow the physical sequence of displacements described in the previous section, namely we start with a water-wet, water-saturated porous medium, then oil displaces water and the wettability changes, and then water displaces oil. Displacement proceeds by a discrete sequence of events. An event is when the generic fluid configuration in one pore or throat changes.

We assume flow at an infinitesimal flow rate where the viscous pressure drop across the network is negligible and capillary forces completely control the fluid configurations. Consider a definite example—oil invasion into a water-filled water-wet porous medium, or primary drainage. There are some throats connected to a reservoir of injected fluid—called the inlet, and some throats connected to another reservoir full of displaced fluid—called the outlet. Initially, all the pores and throats are completely filled with water. However, the throats connected to the inlet are adjacent to a reservoir full of oil. We assume that the water pressure throughout the network is held at some constant reference pressure. We compute the oil pressure necessary for any of the inlet throats to fill with oil. To do this we use the Young–Laplace equation to find the pressure difference between oil and water necessary for a meniscus of oil to penetrate the throat. The Young–Laplace equation is:

$$P_{\mathrm{cow}} = P_{\mathrm{o}} - P_{\mathrm{w}} = \sigma_{\mathrm{ow}}\left(\frac{1}{r_1} + \frac{1}{r_2}\right) \tag{1}$$

where σ_{ow} is the oil/water interfacial tension and r_1 and r_2 are the principal radii of curvature of the interface. We also know the contact angle at which the oil/water interface hits the solid surface. This is sufficient information to compute a capillary pressure for any shape of pore and any contact angle. For simplicity though, consider, to begin with, that all the pores and throats have a circular cross-section. In this case the capillary pressure from Eq. (1) is simply:

$$P_{\mathrm{cow}} = P_{\mathrm{o}} - P_{\mathrm{w}} = \frac{2\sigma_{\mathrm{ow}}\cos\theta_{\mathrm{ow}r}}{R} \tag{2}$$

where R is the radius of the pore or throat and $\theta_{\mathrm{ow}r}$ is the contact angle (the r refers to the receding angle to distinguish it from the advancing contact angle in water invasion). In most cases we can further assume that the system is strongly water-wet and $\cos\theta_{\mathrm{ow}r} = 1$ in Eq. (2).

We fill pores and throats in order of capillary pressure, Eq. (2). This represents filling the pore and throat with the lowest possible oil pressure. For the first displacement, this will be the largest throat connected to the inlet. The throat is filled with oil—the fluid configuration changes from a throat full of water to one full of oil. The next element to be filled could either be the next largest throat connected to the inlet, or the pore adjacent to the throat just filled. The process continues—at every step in the displacement one pore or throat is filled with oil. This pore or throat is adjacent to either the inlet or an already oil-filled element and has the lowest entry capillary pressure given by Eq. (2). Overall the capillary pressure increases as smaller and smaller elements are filled. However, the capillary pressure can decrease between two displacements—in particular after filling a throat, the adjacent pore will be filled at a lower capillary pressure since it will have a larger radius. This is an invasion percolation process [92] and models invasion at an infinitesimally low flow rate, where all the oil/water interfaces are frozen in place by capillary forces with the exception of one moving interface in the element that is being filled. Strictly speaking, when the capillary pressure decreases, oil could retract from some elements to satisfy a new position of capillary equilibrium [93]. However, the fluid configuration is strictly equivalent to the low flow rate limit of invasion whenever the capillary pressure reaches a new maximum.

If we considered pores and throats with different shapes, such as those with a triangular cross-section, the method would be exactly the same. The only difference is that in place of Eq. (2) a more complex relation would be used [10], which would mean that the pores and throats would no longer fill strictly in order of size. However they would still fill in order of capillary pressure. Once oil had filled the center of an element, water would remain in the corners, as shown in Fig. 3. Here and later the expression 'filled' refers to the center of the pore space. An element is filled with a phase if that phase occupies the center of the element, but it is not necessarily completely full of a single fluid, since wetting phase may reside in the corners. The amount of water in the corners is computed from the capillary pressure of the last element to be filled—this prevailing capillary pressure is applied to *all* the pores and throats to determine the curvature of any oil/water interfaces. Eq. (1) is used to find the curvature r_1 of the oil/water interface in the corners. It is normally assumed that r_2—the curvature longitudinal to the element—is infinite. At this stage we do not consider trapping of water, since we assume it can always escape through wetting layers.

Oil invasion continues until some specified maximum capillary pressure or minimum water saturation is reached. Notice that in this model, zero water saturation can be reached if the capillary pressure is allowed to become arbitrarily large. Often experimentally irreducible saturations of up to 30% are observed for reservoir rocks, even if the capillary pressure reaches several atmospheres, representing pore sizes down to fractions of a micron across [94]. The reason for this is the presence of clays and microporosity in the pore space which remain water saturated even for very large capillary pressures. Clays are modeled by assigning a clay volume to pores and throats that remains full of water throughout the displacement [10].

2.5. Waterflooding

After primary drainage we assume that the oil pressure is held constant at the outlet and water is injected slowly from the inlet. Overall the capillary pressure decreases. The filling process is more complex now with five distinct processes. The first is piston-like filling in throats. This is exactly the opposite of oil invasion considered before. However, the computation of the relevant filling capillary pressure is more involved, since water is invading a throat that also contains water in the corners that swell as the water pressure increases [10,33]. The second process is piston-like filling of pores. The complexity here is that the critical radii of curvature for pore filling depends on the number of adjacent throats that are also water-filled. In the literature empirical expressions are used for the capillary pressure for pore filling [77,89]—to date no exact results have been derived based on a realistic pore–throat geometry. The third filling process is snap-off [73,94]. Snap-off only occurs if piston-like filling is not topologically possible, meaning that there is no adjacent water-filled element. Snap-off occurs when the water layers in the corners swell until the layers in two corners meet and there is no longer an oil/water/solid contact. At this point the oil/water interface is unstable and the pore or throat spontaneously fills with water. Snap-off occurs at a positive capillary pressure (a lower water pressure than oil pressure). This is only possible if:

$$\theta_{\mathrm{owa}} < \frac{\pi}{2} - \alpha_{\min} \tag{3}$$

where θ_{owa} is the advancing (water invasion) contact angle in the element and $\alpha_{\min}$ is the smallest half-angle of the corners in that element. The fourth process is forced snap-off. This is analogous to snap-off, but is a forced process, occurring at a negative capillary pressure [77,89]. As the water pressure increases, the curvature of the oil/water interfaces in the corners will change in accordance with Eq. (1). However, the oil/water/solid contact cannot move until the contact angle reaches θ_{owa}. This means that the curvature varies with the capillary pressure, but the oil/water/solid contact remains in the same place—the interface is pinned—with the contact angle varying as a function of capillary pressure. If Eq. (3) is not satisfied, the oil/water interface

will bulge out into the oil—the capillary pressure will be negative—until the contact angle reaches θ_{owa} and the contact begins to move. Any movement of the contact will tend to make the local capillary pressure less negative, drawing in water from nearby and resulting in the spontaneous filling of the element with water. The fifth process is not a displacement as such, but is the collapse of an oil layer. As mentioned briefly above, if an element is filled by piston-like advance then water fills the center of the pore space. Water also resides in the corners, but there may be a layer of oil in between. An oil layer is possible in a corner if:

$$\theta_{owa} > \frac{\pi}{2} + \alpha \tag{4}$$

The water in the pore center is bulging into the oil, as is the water in the corner. As the capillary pressure decreases (becomes more negative) the oil layer thins as the two oil/water interfaces approach each other. When the two interfaces touch we assume that the oil layer spontaneously collapses. The collapse of an oil layer in a single corner can be treated as a separate displacement process.

We have the following generic fluid configurations: (a) an element completely filled with water; (b) an element filled with oil with water in the corners (Fig. 3(a)); and (c) an element filled with water, but with oil layers in one or more corners (Fig. 3(b)—configurations with different numbers of corners with oil layers are treated as separate). A displacement is a process that changes the generic configuration of a pore or throat, and is one of the five processes described above. We know the configuration of each element at each stage. We compute the capillary pressures for all possible displacements, taking into account, where appropriate, the configurations of adjacent elements. We rank all possible configuration changes for all possible elements in a sorted list. For waterflooding the configuration change that has the highest capillary pressure (corresponding to the lowest water pressure) is the next change to occur. We update the configuration of the element selected, and recompute the capillary pressures for displacements for that element and adjacent elements. Then we rearrange the sorted list as necessary to preserve the rank order of pressures. We then continue the process as before.

The algorithm outlined above is deliberately couched in rather general terms and can be applied to other types of process, such as gas injection and the re-injection of oil. All that is needed is to compute the relevant capillary pressures for each displacement and to place them in a sorted list. Configurations are changed in order of capillary pressure and the sorted list is updated as necessary. The expressions for capillary pressure may be algebraically involved (we have deliberately omitted them from this treatment for clarity) and a large number of different configurations may be considered (see the discussion of three-phase flow below), but conceptually the filling sequence is easy to determine.

There is one more complexity—trapping. During waterflooding, oil can be completely surrounded by water and cannot be displaced. To account for this, before a change in configuration is accepted, it has to be checked to see if there is a connected path for the displaced fluid to escape from the candidate element to the outlet. Oil can be connected through oil-filled elements or through elements containing one or more corners with oil layers. An elegant way to deal with this is to assign each phase in each element to clusters. The inlet cluster contains oil or water connected to the inlet —nearest neighbors are then available for piston-like filling. The outlet cluster contains oil or water connected to the outlet and which can be displaced. Isolated clusters are trapped and the oil or water in them cannot be displaced. The assignment of clusters is readjusted after each configuration change. This becomes important during simulations of oil re-injection. Here, water filling pore centers may be trapped, surrounded by oil-filled elements and oil layers. Trapped oil may be reconnected when oil enters an element that is adjacent to a trapped cluster. Piston-like advance from all the elements in the reconnected cluster is now possible and the sorted lists have to be updated accordingly.

Once all the expressions for capillary pressure have been found and the different configurations determined, it is possible to define a unique filling sequence for different types of invasion process. For each process, a sorted list ranks all the capillary pressures for configuration changes. Cluster labeling identifies trapping and reconnection.

2.6. Computing relative permeability

The next step is to compute saturation, capillary pressure and relative permeability. Saturation is easily found. If V_{ip} is the volume of phase p in element i (including the water volume in clay) then the saturation of phase p is given by:

$$S_p = \frac{\sum_{i=1}^{n_e} V_{ip}}{\sum_{i=1}^{n_p} \sum_{i=1}^{n_e} V_{ip}} \tag{5}$$

where n_p is the number of phases (two for oil/water flows) and n_e is the total number of pores and throats.

The capillary pressure is simply the capillary pressure associated with the last configuration change. Defined this way, the capillary pressure during a displacement process varies non-monotonically. To compare with experimental results, where the capillary pressure is imposed on a sample and increases or decreases monotonically, capillary pressure can be defined as the maximum capillary pressure obtained for oil injection, or the minimum capillary pressure for water injection.

To compute absolute and relative permeability, conductances of each phase in each element need to be specified. The conductance of phase p in an element, g_p can be defined as follows:

$$Q_p = g_p \Delta P_p \tag{6}$$

where ΔP_p is the pressure drop across the element and Q_p is the flow rate of phase p (measured in units of volume per unit time). For instance, if the element is a circular cylinder of length L and radius R completely filled with phase p, then from Poiseuille's law:

$$g_p = \frac{\pi R^4}{8\mu_p L} \tag{7}$$

where μ_p is the phase viscosity.

For elements with a triangular geometry where multiple phases are present, the expressions for the conductance (as for capillary pressure) are more involved. Normally exact analytic results are not possible, and empirical expressions are derived from solutions of the Stoke's equation for flow in pores of different geometries and for different fluid configurations [10,29,32,33,95]. One complication for multiphase flow is that due to momentum transfer across the fluid interfaces, the pressure gradient in one phase may affect the flow rate in the other. Furthermore, the conductances as defined by Eq. (7) depend on the boundary condition at the fluid interface [29]. We will not consider this complication further, but when wetting layer flow is important, these effects can be significant and have been quantified in network modeling studies [96].

We now solve for the pressure everywhere in the network and use this information to compute absolute and relative permeability. The pressure of each phase is computed separately, assuming that all oil/water interfaces are frozen in place. Since we are considering displacement at an infinitesimal flow rate, any pressure drops across the network due to flow are assumed to be negligible in comparison with any capillary pressures. Constant pressures are assigned at the inlet and outlet. Sometimes to avoid end effects, these constant pressures are assigned at locations within the network [38,89]. Conservation of mass is invoked at each pore, which is equivalent to conservation of volume if we assume that the fluids are incompressible:

$$\sum_k Q_{pk}^i = 0 \tag{8}$$

where the sum runs over all throats k connected to pore i. The conductance used to find the flow rate is strictly speaking the conductance between the centers of two pores and is the harmonic average of the conductance of the throat and the connected two half-pores. Thus:

$$Q_{pk}^i = g_{pc}(P_j - P_i) \tag{9}$$

where we assume that throat k connects pores i and j, and:

$$\frac{1}{g_{pc}} = \frac{1}{g_{pk}} + \frac{1}{2g_{pi}} + \frac{1}{2g_{pj}} \tag{10}$$

Eqs. (8)–(10) lead to a series of simultaneous equations for the pressures in the pores that can be solved using standard matrix techniques.

The pressure is normally computed initially when the network is entirely saturated with one phase (generally water). Then the absolute permeability of the network is found from Darcy's law:

$$K = \frac{\mu_p Q_{ts} L}{A(P_{inlet} - P_{outlet})} \tag{11}$$

where Q_{ts} is the total flow rate across the network for single-phase flow (this is the flow summed over all throats connected to the inlet), A is the cross-sectional area of the network model and L is the length of the model.

When multiple phases are present in the network, if flow rates are computed using the same pressure drop as for single-phase flow, then the relative permeability is simply:

$$k_{rp} = \frac{Q_{tm}}{Q_{ts}} \tag{12}$$

where Q_{tm} is the total flow rate for the multiphase situation.

Relative permeabilities are often plotted as a function of saturation. The saturation is computed for the same fluid configuration for which the pressure field was found. Again to avoid end effects, sometimes the saturation is only found for a central region of the network model [38]. Since the computation of relative permeability can be time consuming for large networks, as it involves a matrix inversion, the pressure is generally only computed at intervals, say 20 or 40 times during a displacement, rather than after each filling event.

We have briefly described the conceptual framework for developing a pore-scale model of multiphase flow that accounts for disordered connectivity, different shapes of pores and throats, wetting layer flow, and the effects of wettability. In the next section we show some example results.

2.7. Two-phase results

The characterization of the pore space as a disordered network of pores connected by throats with triangular cross-sections, and the model of wettability described above, are sufficient to make good predictions of multiphase flow properties, such as relative permeability and capillary pressure for water-wet sandstones [10,32]. As an illustration of this approach, Fig. 4 shows measured and predicted relative permeabilities for a Berea sample. The steady-state measurements are taken from Oak [97]. The pore space was geologically reconstructed from thin section analysis by Øren and co-workers [10]. The model

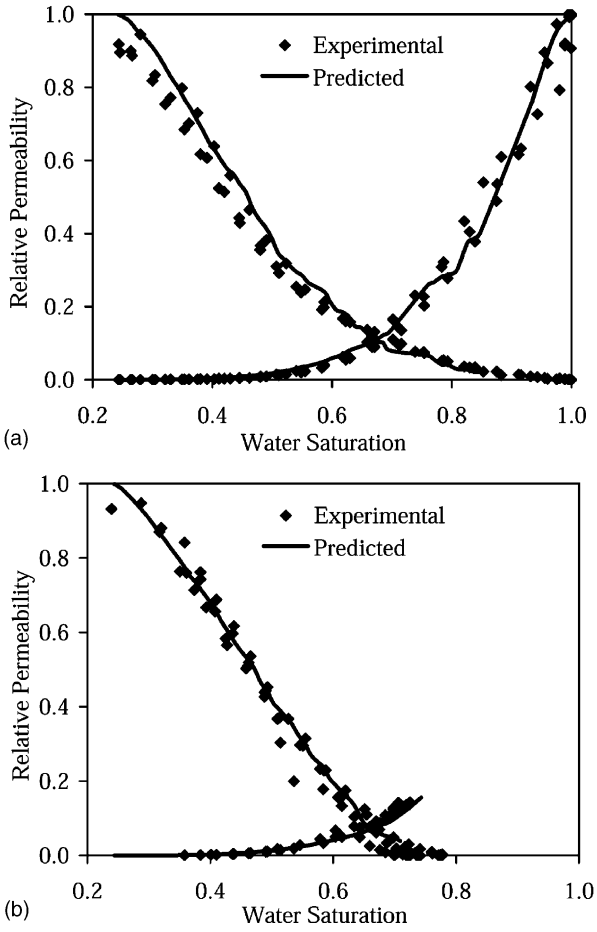

Fig. 4. Predicted and measured oil/water relative permeabilities. The points are from the experimental data of Oak [97] while the solid lines are predictions using the network model illustrated in Fig. 1. (a) Primary drainage: In the network model a receding contact angle of 0 is assumed. (b) Waterflooding: Here a distribution of advancing contact angles, randomly assigned to pores and throats is assumed. Contact angles range from 30° to 90° with a mean of 60°.

is a cube of volume 27 mm^3 containing 12,349 pores and 26,146 throats. A small proportion of clay was introduced into the model. To predict the primary drainage relative permeability, the receding contact angle was everywhere assumed to be zero. For waterflooding, even in water-wet sandstones using refined oils, the advancing contact angle is typically at least 30–60° [94]. Even without the sorption of surface-active material, this apparent contact angle hysteresis is due to roughness on the pore surface, converging/diverging pore geometries [43] or slightly different grain mineralogies [94]. We assumed that the contact angle was likely to be in the range 50–90°, and randomly assigned contact angles in this range to pores and throats assuming a modified Weibull distribution [38]. While this is a plausible distribution of contact angles, there is no a priori way of establishing the exact range of values or the form of the distribution. However, the results did not vary significantly if the distribution of contact angles was changed, as long as the contact angles remained lower than 90° (consistent with a water-wet sample) and had an average larger than 30°.

The predictions of primary drainage and waterflood relative permeabilties shown in Fig. 4 are good. Although these results are promising, predictive modeling of relative permeability for all types of sample for all wettabilities is still a long way off. As we mentioned before, one of the problems with predictive modeling of reservoir rocks is an accurate characterization of wettability. In the literature it is rare to find results for a rock sample where sufficient data for both an accurate pore-space reconstruction and a characterization of contact angles are provided. A hope is that a macroscopic measurement of, for instance, Amott wettability indices [98] would be sufficient to determine an effective contact angle for oil-wet regions and to estimate the proportion of pores that are oil-wet, or to determine a possible distribution of contact angles. For example, Øren et al. [10] tuned the fraction of oil-wet pores to match the observed residual oil saturation, and from that were able to obtain a reasonable prediction of relative permeability for a mixed-wet reservoir sample. Another possibility would be to use NMR response or cryo SEM to determine wettability at the pore scale [94]. However, to date, the model of wettability described in this paper has not been validated through quantitative prediction of relative permeability for non-water-wet samples.

3. Three-phase models

3.1. Three-phase displacement processes

The approach outlined in the previous sections can be extended to three-phase—oil, water and gas—flow. In recent years, many authors have studied this problem using pore-scale modeling [31,38,69,75,76,78,83,99–104]. Three-phase flow occurs during oil migration in the unsaturated zone, oil flow in the saturated zone in the presence of air or other gases, gas injection in oil reservoirs, solution gas drives, reservoir blow-down and steam injection. Potentially this work could be very significant, since direct measurement of three-phase properties, particularly for every type of possible displacement process, is very difficult. The almost universal practice in the oil industry is to estimate three-phase relative permeability from two-phase data using empirical models that have little or no physical basis [105–107]. An alternative approach is to develop physically-based three-phase network models that incorporate all the pertinent pore-scale mechanisms and which are tuned to match available two-phase data. This would significantly improve our understanding of three-phase processes and reduce enormously the uncertainty associated

with the assessment of gas injection projects and the prediction of oil movement in the subsurface. Lerdahl et al. [69] presented a water-wet three-phase model that predicted two- and three-phase relative permeability from Oak [97]. Here we will extend this approach to media of arbitrary wettability and present some preliminary results.

Using the same modeling approach as in the previous sections, Fig. 5 shows the different generic configurations for three phases in elements of equilateral triangular cross-section, extending the work of Blunt and Hui [6,78]. One important feature of three-phase flow is the ability of oil to form a layer sandwiched between water and gas in water-wet and mixed wet pores (Fig. 5(h)–(k)). These spreading layers (so called since they form for systems with a small gas/oil contact angles, corresponding to oils that spread, or nearly spread on water) retain connectivity of the oil phase to very low saturations, leading potentially to high oil recovery during immiscible gravity drainage.

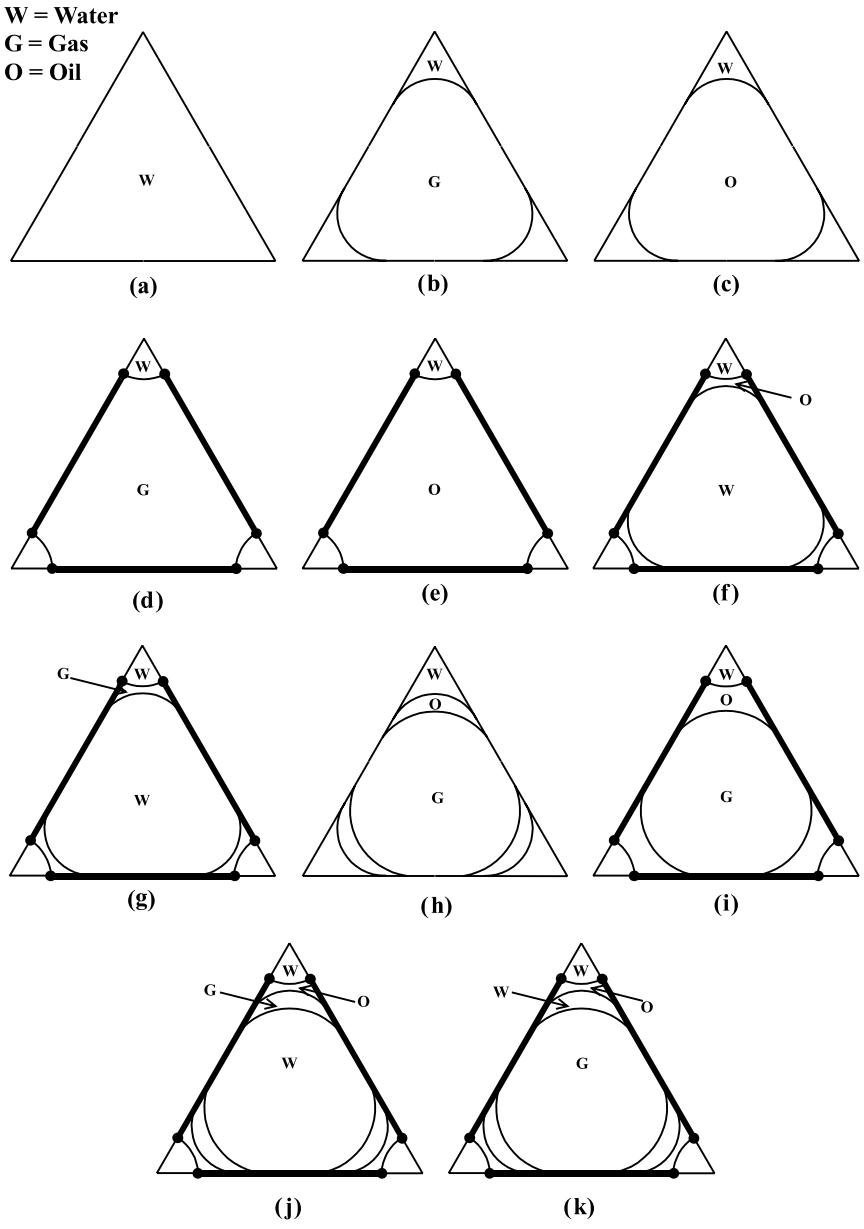

Fig. 5. Different configurations of oil, water and gas in a single pore. As in Fig. 3, the bold line represents surfaces with altered wettability. The dots represent fluid/fluid/solid contacts that are pinned, which means that the contact stays in place as the capillary pressures are changed. For configurations (a)–(c) and (h), surfaces of altered wettability may or may not be present, but the fluid/fluid/solid interfaces are free to move. Exactly what fluid arrangements are present will depend on the contact angles and the capillary pressures. We have assumed that the gas is non-wetting to oil.

We now use the configurations illustrated in Fig. 5 in a network model. A capillary pressure between any two phases P_{cij} is defined as $P_i - P_j$. The capillary pressures necessary for transition from one configuration to another are computed and placed in a sorted list. Displacement proceeds by changing configurations one element at a time, with periodic computation of the pressure field and relative permeabilities.

In three-phase flow, two saturations may be varied independently during a displacement. Thus the saturation path, or more precisely, what phase displaces what, must be specified for each displacement event. There are six possible displacements: oil into water, water into oil, gas into water, water into gas, gas into oil, and oil into gas. Correspondingly there are six sorted lists, ranking the capillary pressures of possible displacements for each of the six processes. Imagine that we specify the invasion of phase i. This means that we consider a displacement event where the volume of i in an element increases. We assume that the pressure of the other two phases j and k are held fixed at a value specified at the last displacement where j and k were the invading phases, respectively. Since the pressures of phases j and k are fixed, P_{cjk} does not change. Phase i can invade either phase j or k. The lowest pressure for phase i for a displacement event is found by comparing the most favorable capillary pressures from the sorted lists for i into j and i into k. Imagine that the capillary pressures obtained for i into j is P_{cij} and for i into k is P_{cik}. If

$$P_{cik} > P_{cij} + P_{cjk} \tag{13}$$

then a displacement of i into j is considered, otherwise i into k. If the event is allowed (no trapping) then it takes place and the pressure of i is updated. If it is not allowed, the event is taken off the sorted list and the top two elements of the i into j and i into k lists are again compared. Thus if a series of invasions is specified by the user, it is possible to define a unique sequence of configuration changes and corresponding saturations, capillary pressures and relative permeabilities.

3.2. Three-phase results

Figs. 6–8 show relative permeabilities and capillary pressures for gas injection. We use the same Berea network as in our two-phase studies. We first simulate primary drainage to a connate water saturation of 20%, then waterflooding to some initial oil saturation S_{oi}, followed by gas invasion. During gas injection we hold the oil/water capillary pressure constant at its value at the end of waterflooding. Unlike our two-phase simulations, we assign a fixed contact angle during waterflooding $\theta_{ow} = \theta_{owa}$ to all surfaces contacted by oil. We study two cases: (i) $\theta_{ow} = 60°$ and $S_{oi} = 0.60$; and (ii) $\theta_{ow} = 180°$ and $S_{oi} = 0.61$.

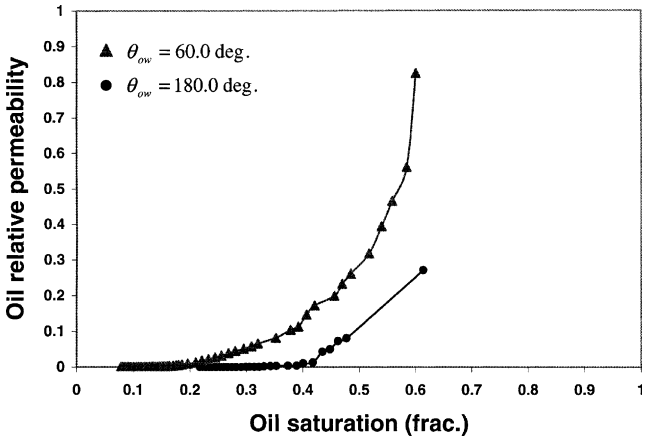

Fig. 6. Gas injection three-phase relative permeabilities. In this and Figs. 7 and 8 the Berea network illustrated in Fig. 1 is used to simulate three-phase flow. The oil relative permeability is shown for gas injection after waterflooding for media of two different wettabilities.

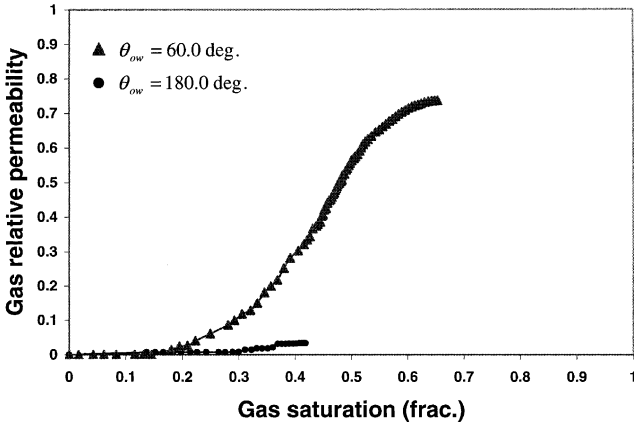

Fig. 7. Three-phase gas relative permeabilities for the same cases as shown in Fig. 6.

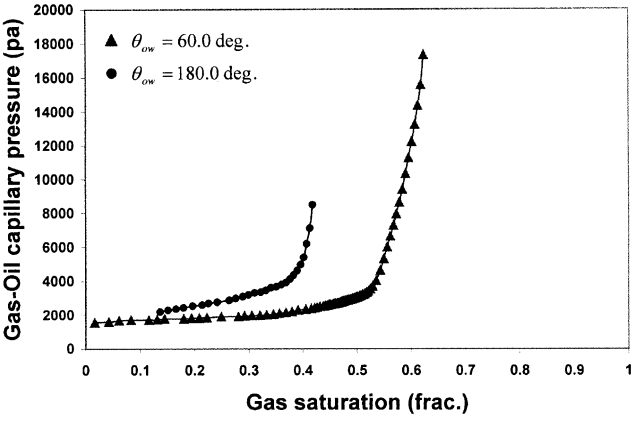

Fig. 8. Three-phase gas/oil capillary pressure for the same cases as shown in Fig. 6.

We need to specify contact angles between oil and water, θ_{ow}, gas and oil, θ_{go}, and gas and water,

θ_{gw}—however, only two of these angles are independent. By considering the horizontal force balance of all three possible fluid/fluid contacts on a solid surface, the following relation between the contact angles and interfacial tensions is obtained [108–110]:

$$\sigma_{gw}\cos\theta_{gw} = \sigma_{go}\cos\theta_{go} + \sigma_{ow}\cos\theta_{ow} \quad (14)$$

In our model we assume $\theta_{go} = 0$. Then with $\sigma_{gw} = 67$ mN/m, $\sigma_{ow} = 48$ mN/m and $\sigma_{go} = 19$ mN/m, we find $\theta_{gw} = 50°$ for $\theta_{ow} = 60°$ and $\theta_{gw} = 116°$ for $\theta_{ow} = 180°$. There is one subtlety though—Eq. (14) is derived assuming static contacts and we apply it to contact angles for moving interfaces. In particular, in Eq. (14) we assume that water is advancing over oil, while receding over gas, and oil is receding over gas. Note that for the oil-wet case ($\theta_{ow} = 180°$) θ_{gw} is greater than 90°, meaning that water is non-wetting to gas.

In these simulations, gas principally displaces oil. Initially oil layers are present and the oil is connected. However, as the gas/oil capillary pressure increases (see Fig. 8) the oil layers collapse, allowing oil to become trapped. Furthermore, for the oil-wet case, water as the non-wetting phase can be trapped in the centers of the pore space by both oil and gas. A phase is trapped if there is no continuous path of that phase to the outlet. This path can be through the centers of the pore space, through spreading layers, or (for water) through wetting layers in the corners of the pores.

The oil relative permeability for the oil-wet medium is lower than for the water-wet case (Fig. 6). If oil is the wetting phase it will reside in the smallest pore spaces, which have a low conductance. In contrast, for a water-wet system, the oil occupies larger pores and has a higher relative permeability at the same oil saturation.

The gas relative permeability for the oil-wet system, Fig. 7, is very low—much lower than for the water-wet case. The reason for this is that in an oil-wet system, the gas is not the non-wetting phase and is forced to occupy pores of intermediate size with a poor connectivity. This effect of wettability on relative permeability is a direct consequence of the constraint on contact angles, Eq. (14) and has been observed experimentally [111–113]. Also the gas/oil capillary pressure for the oil-wet system reaches high values at a lower gas saturation than for the water-wet case (Fig. 8). This is due to trapping of the water phase, which does not occur for a water-wet system.

While many of the qualitative aspects of the results correspond to trends observed experimentally, there is one puzzling feature. We find a trapped oil saturation of around 7% for the water-wet medium and approximately 20% for the oil-wet case. This is due to the collapse of oil layers as the gas/oil capillary pressure increases. However, experimentally oil saturations as low as 0.1% can be reached during gas displacement [94,109,111,112]. Furthermore, at these low saturations, the theoretical explanation is that the oil is flowing in connected layers. The hydraulic conductance of the oil is proportional to the layer area squared, leading to an oil relative permeability that is proportional to the square of the oil saturation [76,114], as seen experimentally for both water-wet and mixed-wet media [111,112,115,116]. We discuss possible reasons for not observing this oil layer drainage below.

One unique feature of three-phase flow that we have ignored in our model is multiple displacement [38,117–120]. An invasion of phase j by phase i may be composed of a displacement of k by i followed by a displacement of j by k. If all the phases are continuous, this is equivalent simply to two separate events. However, the intermediate phase in the displacement—k—may be trapped. In this case disconnected clusters of phase k can rearrange themselves in the pore space, and may reconnect, simply due to capillary forces, when one phase invades part of the cluster than in turn displaces the third phase. This is a double displacement process and has been observed in micromodel experiments [117,118,120] and coded into network models [38,69]. Multiple displacements, involving more than one intermediate stage, are also possible if two phases are trapped. A cascade of disconnected blobs nudge each other before a final displacement of a connected phase [119]. The algorithm for considering such events is somewhat involved, since multiple events for all clusters need to be considered together with the conservation of volume when the cluster moves [119]. Ignoring multiple displacements might explain the trapping of oil, but for gas injection this is unlikely to be a significant effect [119].

3.3. Self-consistency in three-phase flow

The macroscopic equations for flow assume that the relative permeabilities and capillary pressures are functions of saturation only [94]. However, our example results and the discussion above has demonstrated that the macroscopic flow properties depend on the whole saturation history: the saturation and pressure reached during primary drainage that determines wettability alterations; and whether oil, water or gas is the displacing phase. The traditional approach to this problem is to use a single set of relative permeability and capillary pressure curves in numerical models to simulate a given displacement.

For example, waterflood relative permeability curves starting from the known initial water saturation are used to simulate water injection in a reservoir. This will give satisfactory predictions of flow as long as other processes, such as oil or gas injection are not modeled with the same relative permeabilities.

In macroscopic simulations of three-phase flow it is not possible a priori to determine a saturation history for which relative permeabilities and capillary pressures

may be predicted or measured. This causes a problem for the traditional approach of assuming some fixed set of macroscopic flow parameters for a given displacement. To understand this, consider the three-phase results presented above. We assumed that locally the gas saturation increased as the saturations of oil and water decreased while maintaining a fixed oil/water capillary pressure. However, it is known from experimental measurements and numerical simulations, that for gas injection into oil and water after waterflooding, the sequence of saturation changes is rather different [94,116,121]. Gas preferentially displaces oil and this oil is swept ahead of the gas in a so-called oil bank. Thus at a fixed location, the first flooding event is oil invasion into water with a corresponding increase in the oil/water capillary pressure. Gas then invades oil at an initially high saturation and there is very little direct displacement of water by gas. This is a different displacement history, with correspondingly different relative permeabilities [38]. So, for a given set of macroscopic boundary conditions—the rates of gas and/or water injection at the wells and the initial saturation in the reservoir—what is the appropriate local sequence of displacements or saturation path? The saturation path depends on the three-phase relative permeabilities, as shown in numerous simulation studies (see, for instance [122,123]). But, the relative permeabilities, from network modeling, depend on the saturation path! It thus appears impossible to define a sequence of displacements for the network model without somehow first knowing the relative permeabilities.

The way out of this impasse is to develop a self-consistency procedure [76]. A saturation path is guessed and the network model run is performed where the displacement sequence mimics the imposed saturation path as closely as possible. Then the relative permeabilities computed for this path are tabulated as a function of a phase saturation that varies monotonically during the displacement (say gas saturation, for gas invasion). These relative permeabilities are then used in a one-dimensional numerical simulator to compute the local sequence of saturation changes. If this sequence is different from the one imposed on the model, the new saturation path is used to define another simulation for the network model from which a new set of relative permeabilities are computed. This procedure continues until the network model computes relative permeabilities for a saturation path which is the same as the path obtained from a large-scale numerical solution for three-phase displacement with the boundary conditions of interest. This method normally converges in around five iterations [76].

In previous three-phase network model studies on water-wet media, the self-consistency procedure resulted in a saturation path where oil layers remained stable and a characteristic layer drainage regime to low oil saturation was observed [76]—the trapping of oil evident in Fig. 6 is a consequence of forcing a fixed oil/water capillary pressure which may not be representative of a real displacement.

To recap: relative permeability and capillary pressure used in macroscopic flow equations depend on the whole saturation history. It is not feasible experimentally to measure these properties for every possible displacement path. This is a particular problem in three-phase flow where there are an infinite number of possible displacement paths for given initial and injection conditions. A way around this problem is to use a physically-based modeling approach that finds macroscopic properties consistent with the displacement of interest. The models can be verified against available experimental data and then used to predict behavior outside the range probed experimentally.

A more general approach to this problem is to consider a large-scale simulator where relative permeabilities are not simply tabulated as functions of saturation, as in conventional methods, but where each grid block in the simulator has a network model associated with it. At the beginning of a time-step the network model computes three-phase relative permeabilities and capillary pressures using the existing configuration of phases. These are then used in a conventional explicit finite-difference or finite-element code to compute the pressure field and to transport fluid between grid blocks. Each of the grid blocks now has new saturations. The network model then undergoes a series of displacements to reach these new saturations. The relative permeabilities are then recomputed and the process is repeated. This procedure automatically generates self-consistent relative permeabilities, while providing a macroscopic prediction of the flow behavior. The concept of coupling different scales of simulation together is discussed further in the section on field-scale consequences below.

4. Dispersion, dissolution and electrical properties

In this paper we have described a framework for pore-scale modeling of multiphase flow processes. However, the prediction of relative permeability and capillary pressure for quasi-static displacements is not the only problem of interest. In essence, the model computes the pore-scale configuration of phases for different displacement sequences. This information can be used to study a variety of other phenomena. For instance, for understanding interfacial mass transfer, vital in determining dissolution and vaporization rates of contaminants in polluted soils, the interfacial area pays a critical role. Recently quasi-static pore-scale models have been used to compute interfacial area and common lines as a function of saturation and capillary pressure [18,23]. In addition, the concentration of a solute in water can be

computed in the pore space. The approach is very similar to that used for computing relative permeability—conservation of mass in each pore is invoked and Fick's law combined with convection is used to relate the flow rate of contaminant to concentration and pressure gradients. This then leads directly to an estimation of dissolution rates of components originally in the oil phase [16–23]. By tuning the pore-size distribution to match capillary pressure data, and by incorporating a model of dissolution across wetting layers [16], good predictions of laboratory data were made [17]. Other work involving mass transfer, where a concentration field is computed in one of the phases in the network, include studies of drying processes [24], solution gas drives [124,125], gas condensate systems [83,84,126], water vapor transport [25], evaporation of a binary liquid [26] and dispersion [22,127].

The main challenge in this field is to combine a model of the multiphase fluid configuration with a computation of transport processes within and between phases. The approximations and assumptions used to describe the pore space relevant for understanding relative permeability and capillary pressure may no longer be adequate for the understanding of other processes. For example, in Ref. [127], a semi analytic model was used to describe the single-phase flow field in a two-dimensional network of pores with square cross-section. Particle tracking was then used to study dispersion in the network. In principle this work could be extended to study dispersion and transport in multiphase systems. However, the model of wetting phase in the corner of triangular pore elements, while it may be adequate to describe flow, may no longer be sufficient to describe dispersive transport. Similarly, predictions of interfacial areas and mass transfer between phases, based on the picture of fluid arrangement described in this paper, may not be quantitatively accurate. This is something that has yet to be explored, since first-principles predictive modeling of mass transfer and transport processes has not yet been attempted.

Studies of electrical resistance have applications in core analysis and logging, where the electrical properties of rocks in the near well-bore region can be readily studied, in contrast to multiphase flow parameters that can only be determined from time-consuming measurements on cores extracted from the reservoir. By combining flow and electrical properties in a single consistent pore-scale model, it is hoped to be able to predict the flow properties of the reservoir from its electrical response. Oil is considered to be an insulator, but the water conducts. The approach to finding the overall conductance of the model is similar to that for finding relative permeability, but where the electrical conductance of each element is simply proportional to the cross-sectional area of water [11–13,15]. Again the challenge here is to combine the computation of several different properties in a single model, and to use different pieces of experimental data to validate or tune a network model, and then to use it to predict other, more difficult to measure, properties.

5. Rate-dependent effects

There are several circumstances where the approximation of quasi-static displacement is not valid. Examples include: fracture flow, where flow rates may be very large—often of the order of hundreds of meters a day; displacements with very low interfacial tensions that substantially reduce capillary forces, such as near-miscible gas injection, gas condensate reservoirs and surfactant flooding; near well-bore flows; flows involving polymers, gels and foams where very large pressure gradients are found; and some cases where wetting layer flow and formation is significant, such as spontaneous wetting into a dry soil. In all these cases, capillary and viscous forces both control the fluid configurations at the pore scale. As a consequence, macroscopic flow properties, such as relative permeability, are functions of flow rate, leading to a Darcy law where flow rate is nonlinearly dependent on pressure gradient.

The ratio of viscous to capillary forces is defined by a capillary number [94]:

$$N_c = \frac{\mu q}{\sigma} \tag{15}$$

where σ is the interfacial tension and μ is the viscosity of the injected phase. q is the flow rate measured in units of volume per unit time per unit area. For slow flows away from wells, typical capillary numbers are in the range 10^{-6}–10^{-10}, representing a ratio of capillary pressure to a viscous pressure gradient across a single pore of around 1000 or higher. A single pore-filling event normally occurs in fractions of a second (as observed, for instance, in micromodel studies, [94]). In contrast, it may take several days to years for a displacement sequence to be completed at a given location in a natural setting. Thus the assumption that in a network model, containing a few thousand pores, that only one pore is filled at a time, appears to be reasonable. However, at high flow rates or fluid viscosities or low interfacial tensions, this approximation will break down.

Rate dependent pore-scale modeling is qualitatively dissimilar to quasi-static approaches. In quasi-static modeling a capillary pressure is imposed over the entire network. This is used to define the fluid configuration in each element and the corresponding volumes of each phase. Pores and throats change their configuration one at a time. The computation of the pressure, although necessary to find the relative permeability, does not affect the displacement sequence. In dynamic pore-scale modeling the approach is different and more akin to conventional macroscopic simulation models. Here the

volumes of each phase in each element are known. From this the configuration of the phases in the element is derived together with the local pressure difference between phases (the capillary pressure, but now it varies with position and is distinct from its macroscopically averaged counterpart) and the conductance of each phase. In contrast to quasi-static models, the pressure is computed by invoking mass balance summed over *all* phases and assuming that all the fluid interfaces are potentially mobile. Separate pressure computations for each phase are not made—instead the pressure in the water is computed, with the pressures of the other phases found from the local capillary pressure. Then the volumes of each phase in each element are updated, using the flow rates from the computed pressure field. Usually a very small time-step is chosen, so that the generic configuration of fluid in only a single element changes. Many authors have used this approach to study rate-dependent effects in drainage, imbibition and the mobilization of trapped oil ganglia (see, for instance, [39,40,128,129]). However, to date nobody has accurately studied rate effects involving wetting and spreading layers, and in particular how they swell and initiate snap-off during wetting phase invasion. One reason, despite the apparent conceptual simplicity of dynamic models, is the difficulty of accurately representing discrete pore filling events for moderately slow flow rates, corresponding to capillary numbers of about 10^{-4}. The pressure needs to be solved several times for each element filled, even for drainage processes [130]. For imbibition, the process is time consuming even when approximations are made about the flow in wetting layers [128]. Instead, most authors have resorted to rather simplistic treatments of layer flow, such as assuming a fixed conductance in wetting layers throughout the displacement [75,79–81,131].

The spontaneous wetting of a dry or nearly dry soil represents one of the most fundamental and conceptually simple processes in porous media, and is an example where a dynamic pore-scale modeling approach is necessary. At the beginning of the displacement, viscous and capillary forces are of the same order of magnitude, and wetting layers form and swell in advance of an invading water front. Despite much work on this and related processes, such as capillary fingering in porous media and fractures [79–81,131,132], a full treatment of this fascinating problem has not yet been presented.

6. Field-scale consequences of pore-scale physics

The emphasis in this paper has been on predictive modeling of multiphase flow properties. However, this work is limited to cases where a detailed characterization of the pore space is possible, combined with an accurate assessment of wettability. In most field situations, the major problem is characterizing flow properties in highly heterogeneous environments based on scant experimental data from core samples that may only be representative of a very small portion of the reservoir.

Network modeling could be used to assign multiphase flow properties to detailed fine-scale geological models. For single-phase properties—porosity and permeability—geological models populated with values representing known data, combined with a plausible statistical inference of spatial variability, are now routinely generated for large hydrocarbon reservoirs. Pore-scale modeling has a rather limited role in these studies, since it is easy to measure permeability and porosity on a large number of samples and thus to relate different rock types and geological structures to flow parameters. Multiphase flow is different, since measurements are much more scarce and there is no easy way of estimating trends in relative permeability and capillary pressure. At present a single set of relative permeability curves are normally applied to the whole field, or to each major rock type. The curves themselves often come from measurements of doubtful quality, where the wettability and pore structure may be atypical of the field.

An alternative approach is to use pore-scale modeling to predict a small number of good-quality measurements for which pore structure and wettability information are also available. Then to use this model, validated against available experimental evidence, to predict variations in multiphase flow properties as, for instance, wettability and grain size distribution are varied.

While recovery is strongly influenced by well placement and the location of the largest-scale geological structures, as we show in the example below, for systems with significant wettability variation, the recovery is extremely sensitive to relative permeability. For three-phase flow, the correct assignment of relative permeability, particularly at low oil saturation may be very uncertain, and can have a huge impact on predictions of oil recovery [105].

To illustrate how pore-scale modeling could be used in future as a tool in reservoir characterization, we consider a simple two-dimensional homogeneous system. The reservoir is tilted and the bottom is completely saturated with water (it lies at the oil/water contact, defined as where the oil/water capillary pressure is zero). With height above the oil/water contact, the water saturation decreases in the capillary transition zone, and at the top of the system reaches its irreducible or connate value. We then consider waterflooding the reservoir using a well perforated along the lower side of the reservoir, while oil is produced along the higher side. At the pore scale, we assume that wherever the oil directly contacts solid, the solid surface becomes strongly oil-wet with an advancing oil/water contact angle distributed between 150° and 180°. However, near the oil/water

contact, since the water saturation is high, most of the pore spaces will remain water-wet. There is a wettability transition – the medium becomes more oil-wet with height above the oil/water contact. This type of variability is quite common and is observed, for instance, in Prudhoe Bay in Alaska [133]. Waterflooding is then simulated using a conventional finite-difference reservoir simulator. Depending on height, waterflooding will start from different water saturations and in media of different wettability. Different relative permeabilities are used for different heights and are obtained from pore-network modeling of waterflooding from the correct initial water saturation and wettability. We assume that this is an adequate representation of the large-scale flow. The present state-of-the-art for such modeling is to use empirical hysteresis curves to represent waterflooding relative permeabilities starting at different initial water saturations. These curves extrapolate the relative permeabilities from measurements for a system drained to connate water saturation and then waterflooded to residual oil. The model most widely used in the petroleum literature is due to Killough [134] and was implemented in this study.

Fig. 9 shows the drainage and waterflood relative permeabilities computed using the pore-scale model with the same Berea sandstone data as before. The drainage curve is also shown in Fig. 4, while the waterflooding curve assumes that all the surfaces contacted by oil become strongly oil-wet. Also shown on Fig. 9 are the relative permeability curves for waterflooding from different initial water saturations computed using our pore-scale model. Notice that the water relative permeabilities lie below the bounding waterflood curve in some cases. The reason for this is the wettability and connectivity of the water at the pore scale. For waterflooding starting at moderate water saturations, water already occupies most of the pores and throats. Because they are the smaller elements in the network, their connectivity and hence relative permeability is low. When waterflooding starts, since all the oil-filled pores are oil-wet, water preferentially fills the larger oil-filled pores. This leads to a rapid increase in water saturation without significantly improving the connectivity of the sub-network of water-filled regions. As a consequence, the relative permeability remains rather low and only increases rapidly once the oil-wet regions are well connected. If the initial water saturation is lower, the same phenomenon is seen, but now shifted to lower water saturation. This allows the water relative permeability to become quite large in the intermediate saturation range. The main point here is that while this can be explained in terms of pore-scale configurations, this behavior is not easy to predict without pore-scale modeling and is difficult to test experimentally, where the only measurements, to date, of such hysteresis have been on uniformly water-wet samples [94,134].

The macroscopic consequences of the two approaches to finding relative permeability are illustrated in Fig. 10.

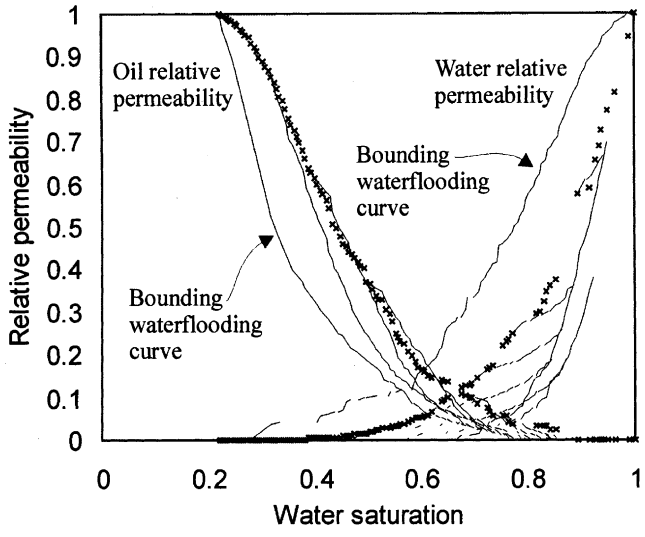

Fig. 9. Predicted relative permeability curves. Results from the pore-scale model using a Berea network, Fig. 1, are shown. The drainage curve (points) assumes an initially water-wet system and is also shown in Fig. 4. The bounding curves are for waterflooding from an irreducible water saturation of 20% where all surfaces contacted by oil are oil-wet. The other curves are waterflood relative permeabilities starting at different initial water saturations. Again all surfaces contacted by oil are strongly oil-wet. Notice that the water relative permeabilities can lie below the drainage curve.

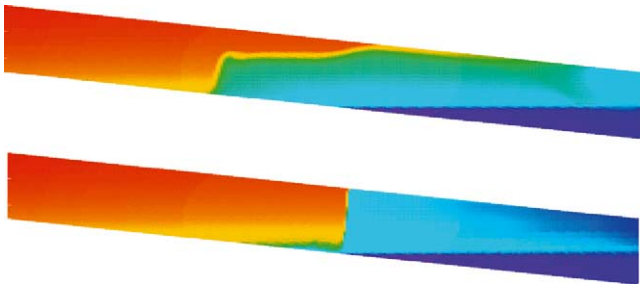

Fig. 10. Simulations of waterflooding. Blue represents 100% water saturation and red irreducible water saturation (20%). Water is injected from the bottom right hand face of a two-dimensional homogeneous reservoir and oil is produced from the left hand face. Initially, the base of the reservoir is entirely water saturated and the water saturation decreases to its irreducible value with height. The upper figure shows a simulation of waterflooding using a conventional model of relative permeability hysteresis based on drainage and waterflooding curves. Essentially the system behaves as though it were entirely oil-wet, with early water breakthrough and poor recovery. Using pore-scale modeling to assign relative permeabilities leads to very different macroscopic behavior (lower figure), even if the drainage and waterflood relative permeabilities are the same. For waterflooding from intermediate relative permeabilities, the water relative permeability is low (see Fig. 9), giving a more uniform sweep of the reservoir and better recoveries. This example illustrates the impact of using physically-based relative permeabilities on macroscopic predictions of oil recovery.

The initial distribution of water saturation with height is found from the drainage capillary pressure curves, which are derived from the network model. The conventional Killough model of relative permeability essentially considers the system to be oil-wet with a large water relative permeability and low oil relative permeability. This leads to early water breakthrough, slow oil production after breakthrough and correspondingly poor recovery. The network model derived relative permeabilities, however, indicate a much more favorable displacement. The low water relative permeability leads macroscopically to a displacement with delayed breakthrough at a low oil saturation. The oil-wet characteristics of the medium also allow a low residual oil saturation to be reached. Had we used the experimentally-derived water-wet curves and the Killough model, the recovery would have been more favorable, but still lower than for the pore-scale model, since for the water-wet case considerable quantities of oil are trapped [135]. Moreover, in this case the waterflood relative permeabilities used would not have corresponded to the wettability state of the reservoir.

While the results are specific to the particular system studied, they do indicate how a physically-based prediction of relative permeability can result in very different macroscopic predictions of oil recovery than the use of more empirical approaches. Were pore-scale modeling to be validated for a wide range of realistic reservoir systems, there is enormous potential to transform multiphase reservoir characterization using network model derived properties to populate simulation models.

An idea for the future is to consider the dynamic coupling of pore-scale modeling with conventional simulation [135]. Heiba et al. [136] was the first to propose this approach, coupling a semi-analytic network model of two-phase flow to a one-dimensional finite-element simulator. In a generalization of this method, each grid block in a three-dimensional reservoir simulator would be coupled to a pore-scale model with a representative wettability and pore structure. The model would mimic the sequence of saturation changes observed at that location and output relative permeabilities and capillary pressures for the next time step. This approach is the same as outlined for a self-consistency procedure for three-phase flow. To prevent the method becoming prohibitively time consuming, it may be possible to have explicit network models for only selected grid blocks, and use the results from these blocks for other similar regions.

7. Conclusions

Pore-network modeling is now a well-established and successful technique for understanding and predicting a wide range of multiphase flow and transport properties, such as relative permeability, capillary pressure, interfacial area and dissolution rate coefficients. With appropriate data, such models can be predictive, offering the possibility of using pore-scale modeling as a practical tool in reservoir characterization and simulation.

We have briefly presented a conceptual framework for modeling two- and three-phase flow in geologically realistic networks. For a water-wet sandstone we showed that we were able to predict relative permeability. Such models can be used as a platform for studying a variety of different phenomena in porous media, and in recent years there has been an explosion of interest in such studies.

We indicated how pore-scale modeling might be used in the future as a reservoir characterization tool, assigning a plausible spatial distribution of multiphase flow properties to detailed geological models. Through a simple example, we illustrated how physically-derived relative permeabilities can give very different predictions of macroscopic oil recovery from conventional models of relative permeability and hysteresis. Last we proposed a dynamic modeling approach where pore-scale models and larger-scale grid-based simulation are coupled together.

Acknowledgements

The authors are grateful to Pål-Eric Øren for sharing his Berea data with us. The authors also thank the members of the Imperial College consortium on pore-scale modelling (Statoil, Japan National Oil Corporation, Gaz de France, BHP, Schlumberger, Enterprise Oil, PDVSA-Intevep, Shell, the Department of Trade and Industry and the EPSRC) for financial support.

References

[1] Fatt I. The network model of porous media I. Capillary pressure characteristics. Trans AIME 1956;207:144–59.
[2] Fatt I. The network model of porous media II. Dynamic properties of a single size tube network. Trans AIME 1956;207:160–3.
[3] Fatt I. The network model of porous media III. Dynamic properties of networks with tube radius distribution. Trans AIME 1956;207:164–81.
[4] Berkowitz B, Balberg I. Percolation theory and its application to groundwater hydrology. Water Resources Res 1993;29(4):775–94.
[5] Sahimi M. Flow and transport in porous media and fractured rock: from classical methods to modern approaches. Weinheim: VHC; 1995.
[6] Blunt MJ. Flow in porous media—pore-network models and multiphase flow. Curr Opinion Colloid Interf Sci 2001;6:197–207.
[7] Koplik J. Creeping flow in two-dimensional networks. J Fluid Mech 1982;119:219–47.

[8] Jerauld GR, Salter SJ. The effect of pore-structure on hysteresis in relative permeability and capillary pressure: pore-level modeling. Transport Porous Med 1990;5:103–30.
[9] Heiba AA, Sahimi M, Scriven LE, Davis HJ. Percolation theory of two-phase relative permeability. SPE Reservoir Eng 1992;7: 123–32.
[10] Øren PE, Bakke S, Arntzen OJ. Extending predictive capabilities to network models. SPE J 1998;3:324–36.
[11] Man HN, Jing XD. Pore network modelling of electrical resistivity and capillary pressure characteristics. Transport Porous Med 2000;41:263–86.
[12] Man HN, Jing XD. Network modelling of wettability and pore geometry effects on electrical resistivity and capillary pressure. J Petroleum Sci Eng 1999;24:255–67.
[13] Man HN, Jing XD. Network modeling of strong and intermediate wettability on electrical resistivity and capillary pressure. Adv Water Resources 2001;24:345–63.
[14] Tsakiroglou CD, Fleury M. Pore network analysis of resistivity index for water-wet porous media. Transport Porous Med 1999;35(1):89–128.
[15] Tsakiroglou CD, Fleury M. Resistivity index of fractional wettability porous media. J Petroleum Sci Eng 1999;22:253–74.
[16] Zhou D, Dillard LA, Blunt MJ. A physically based model of dissolution of nonaqueous phase liquids in the saturated zone. Transport Porous Med 2000;39(2):227–55.
[17] Dillard LA, Blunt MJ. Development of a pore network simulation model to study nonaqueous phase liquid dissolution. Water Resources Res 2000;36(2):439–54.
[18] Dillard LA, Essaid HI, Blunt MJ. A functional relationship for field-scale nonaqueous phase liquid dissolution developed using a pore network model. J Contaminant Hydrology 2001;48:189–99.
[19] Jia C, Shing K, Yortsos YC. Visualization and simulation of NAPL solubilization in pore networks. J Contaminant Hydrology 1999;35(4):363–87.
[20] Jia C, Shing K, Yortsos YC. Advective mass transfer from stationary sources in porous media. Water Resources Res 1999;35(11):3239–51.
[21] Held RJ, Celia MA. Pore-scale modeling and upscaling of nonaqueous phase liquid mass transfer. Water Resources Res 2001;37(3):539–49.
[22] Ahmadi A, Aigueperse A, Quintard M. Calculation of the effective properties describing active dispersion in porous media: from simple to complex unit cells. Adv Water Resources 2001;24:423–38.
[23] Held RJ, Celia MA. Modeling support of functional relationships between capillary pressure, interfacial areas and common lines. Adv Water Resources 2001;24:325–43.
[24] Yiotsis AG, Stubos AK, Boudouvis AG, Yortsos YC. A 2D pore-network model of the drying of single-component liquids in porous media. Adv Water Resources 2001;24:439–60.
[25] Carmeliet J, Descamps F, Houvenaghel G. A multiscale network model for simulating moisture transfer properties of porous media. Transport Porous Med 1999;35(1):67–88.
[26] Freitas DS, Prat M. Pore network simulation of evaporation of a binary liquid from a capillary porous medium. Transport Porous Med 2000;40(1):1–25.
[27] Kharabaf H, Yortsos YC. Pore network model for foam formation and propagation in porous media. SPE J 1998;3:42–53.
[28] Friedman SP, Seaton NA. Critical path analysis of the relationship between permeability and electrical conductivity of three-dimensional pore networks. Water Resources Res 1998;34(7): 1703–10.
[29] Ransohoff TC, Radke CJ. Laminar flow of a wetting fluid along the corners of a predominantly gas-occupied noncircular pore. J Colloid Interf Sci 1988;121:392–401.
[30] Gunstensen AK, Rothman DH. Lattice Boltzmann studies of immiscible two-phase flow through porous media. J Geophys Res 1993;98(B4):6431–41.
[31] van Kats FM, Egberts PJP. Simulation of three-phase displacement mechanisms using a 2D Lattice–Boltzmann model. Transport Porous Med 1999;37(1):55–68.
[32] Øren PE, Bakke S. Process based reconstruction of sandstones and prediction of transport properties. Transport Porous Med 2002;46: 311–43.
[33] Patzek TW. Verification of a complete pore network simulator of drainage and imbibition. SPE J 2001;6(2):144–56.
[34] Dixit AB, McDougall SR, Sorbie KS. A pore-level investigation of relative-permeability hysteresis in water-wet systems. SPE J 1998;3:115–23.
[35] Dixit AB, McDougall SR, Sorbie KS, Buckley JS. Pore-scale modeling of wettability effects and their influence on oil recovery. SPE Reservoir Evaluation Eng 1999;2:25–36.
[36] Dixit AB, Buckley JS, McDougall SR, Sorbie KS. Empirical measures of wettability in porous media and the relationship between them derived from pore-scale modeling. Transport Porous Med 2000;40(1):27–54.
[37] Fischer U, Celia MA. Prediction of relative and absolute permeabilities for gas and water from soil water retention curves using a pore-scale network model. Water Resources Res 1999; 35(4):1089–100.
[38] Fenwick DH, Blunt MJ. Three-dimensional modeling of three-phase imbibition and drainage. Adv Water Resources 1998; 21(2):121–43.
[39] Blunt M, King P. Macroscopic parameters from simulations of pore scale flow. Phys Rev A 1990;42(8):4780–7.
[40] Blunt M, King P. Relative permeabilities from two- and three-dimensional pore-scale network modelling. Transport Porous Med 1991;6:407–33.
[41] Lowry MI, Miller CT. Pore-scale modeling of nonwetting-phase residual in porous media. Water Resources Res 1995;31(3):455–73.
[42] Bakke S, Øren PE. 3D pore-scale modeling of sandstones and flow simulations in the pore networks. SPE J 1997;2:136–49.
[43] Ioannidis MA, Chatzis I. On the geometry and topology of 3D stochastic porous media. J Colloid Interf Sci 2000;229:323–34.
[44] Tsakiroglou CD, Payatakes AC. Characterization of the pore structure of reservoir rocks with the aid of serial sectioning analysis, mercury porosimetry and network simulation. Adv Water Resources 2000;23(7):773–89.
[45] Pilotti M. Reconstruction of clastic porous media. Transport Porous Med 2000;41(3):359–64.
[46] Liang ZR, Philippi PC, Fernandes CP, Magnani FS. Prediction of permeability from the skeleton of three-dimensional pore structure. SPE Reservoir Evaluation Eng 1999;2:161–8.
[47] Lin C, Cohen MH. Quantitative methods of microgeometric modelling. J Appl Phys 1982;53:4152–62.
[48] Holt RM, Fjoer E, Torsoeter O, Bakke S. Petrophysical laboratory measurements for basin and reservoir evaluation. Marine and Petroleum Geology 1996;13:383–91.
[49] Dunsmuir JH, Ferguson SR, D'Amico KL, Stokes JP. X-ray microtomography: a new tool for the characterization of porous media. In: Paper SPE 22860, Proceedings of the SPE Annual Meeting, Dallas, TX 6–9 October 1991.
[50] Spanne P, Thovert JF, Jacquin CJ, Lindquist WB, Jones KW, Adler PM. Synchrotron computed microtomography of porous media: topology and transports. Phys Rev Lett 1994;73:2001–4.
[51] Hazlett RD. Simulation of capillary dominated displacements in microtomographic images of reservoir rocks. Transport Porous Med 1995;20:21–35.
[52] Coker DA, Torquato S, Dunsmuir JH. Morphology and physical properties of Fontainebleau sandstone via tomographic analysis. J Geophys Res 1996;101(B8: Solid Earth and Planets):17497–506.

[53] Masad E, Muhunthan B, Martys N. Simulation of fluid flow and permeability in cohesionless soils. Water Resources Res 2000;36(4):851–64.
[54] Hilpert M, Miller CT. Pore-morphology-based simulation of drainage in totally wetting porous media. Adv Water Resources 2001;24:243–55.
[55] Vogel HJ, Roth K. Quantitative morphology and network representation of soil pore structure. Adv Water Resources 2001;24:233–42.
[56] Liang ZR, Fernandes CP, Magnani FS, Philippi PC. A reconstruction technique for three-dimensional porous media using image analysis and Fourier transforms. J Petroleum Sci Eng 1998;21:273–83.
[57] Liang Z, Ioannidis MA, Chatzis I. Permeability and electrical conductivity of porous media from 3D stochastic replicas of the microstructure. Chem Eng Sci 2000;55:5247–57.
[58] Ioannidis MA, Chatzis I, Kwiecien MJ. Computer enhanced core analysis for petrophysical properties. J Canadian Petroleum Technol 1999;38:18–25.
[59] Bekri S, Xu K, Yousefian F, Adler PM, Thovert JF, Muller J, et al. Pore geometry and transport properties in North Sea chalk. J Petroleum Sci Eng 2000;25:107–34.
[60] Quiblier J. A new three dimensional modeling technique for studying porous media. J Colloid Interf Sci 1984;98:84–94.
[61] Yeong C, Torquato S. Reconstructing random media II. Three-dimensional media from two-dimensional cuts. Phys Rev E 1998;58:224–33.
[62] Adler PM, Jacquin CG, Quiblier JA. Flow in simulated porous media. Int J Multiphase Flow 1990;16:691–712.
[63] Adler PM, Jacquin CG, Thovert JF. The formation factor of reconstructed porous media. Water Resources Res 1992;28:1571–6.
[64] Biswal B, Manwart C, Hilfer R, Bakke S, Øren PE. Quantitative analysis of experimental and synthetic microstructures for sedimentary rock. Physica A 1999;273:452–75.
[65] Bryant S, King PR, Mellor DW. Network model evaluation of permeability and spatial correlation in a real random sphere packing. Transport Porous Med 1993;11:53–70.
[66] Bryant S, Blunt MJ. Prediction of relative permeability in simple porous media. Phys Rev A 1992;46:2004–11.
[67] Bryant SL, Mellor DW, Cade CA. Physically representative network models of transport in porous media. AIChE J 1993;39(3):387–96.
[68] Bryant S, Raikes S. Prediction of elastic-wave velocities in sandstones using structural models. Geophysics 1995;60(2):437–46.
[69] Lerdahl TR, Øren, PE, Bakke S. A predictive network model for three-phase flow in porous media. In: SPE 59311, Proceedings of the SPE/DOE Symposium on Improved Oil Recovery, Tulsa, OK, 2–5 April 2000.
[70] Coehlo D, Thovert JF, Adler PM. Geometrical and transport properties of random packings of spheres and aspherical particles. Phys Rev E 1997;55:1959–78.
[71] Thompson KE, Fogler HS. Modeling flow in disordered packed beds from pore-scale fluid mechanics. AIChE J 1997;43(6):1377–87.
[72] Rajaram H, Ferrand LA, Celia MA. Prediction of relative permeabilities for unconsolidated soils using pore-scale network models. Water Resources Res 1997;33(1):43–52.
[73] Lenormand R, Zarcone C, Sarr A. Mechanisms of the displacement of one fluid by another in a network of capillary ducts. J Fluid Mech 1983;135:337–53.
[74] Dullien FAL, Zarcone C, MacDonald IF, Collins A, Brochard RDE. The effects of surface roughness on the capillary pressure curves and heights of capillary rise in glass bead packs. J Colloid Interf Sci 1989;127(2):363–72.
[75] Mani V, Mohanty KK. pore-level network modeling of three-phase capillary pressure and relative permeability curves. SPE J 1998;3:238–48.
[76] Fenwick DH, Blunt MJ. Network modeling of three-phase flow in porous media. SPE J 1998;3:86–97.
[77] Blunt MJ. physically-based network modeling of multiphase flow in intermediate-wet porous media. J Petroleum Sci Eng 1998; 20:117–25.
[78] Hui MH, Blunt MJ. Effects of wettability on three-phase flow in porous media. J Phys Chem B 2000;104:3833–45.
[79] Hughes RG, Blunt MJ. Pore scale modeling of rate effects in imbibition. Transport Porous Med 2000;40(3):295–322.
[80] Hughes RG, Blunt MJ. pore-scale modeling of multiphase flow in fractures and matrix/fracture transfer. SPE J 2001;6(2):126–36.
[81] Hughes RG, Blunt MJ. Network modeling of multiphase flow in fractures. Adv Water Resources 2001;24:409–21.
[82] Ronen D, Scher H, Blunt M. Field observations of a capillary fringe before and after a rainy season. J Contaminant Hydrology 2000;44:103–18.
[83] Wang X, Mohanty KK. pore-network model of flow in gas-condensate reservoirs. SPE J 2000;5(4):426–34.
[84] Wang X, Mohanty KK. Critical condensate saturation in porous media. J Colloid Interf Sci 1999;214:416–26.
[85] Tuller M, Or D, Dudley LM. Adsorption and capillary condensation in porous media: liquid retention and interfacial configurations in angular pores. Water Resources Res 1999;35(7): 1949–64.
[86] Or D, Tuller M. Liquid retention and interfacial area in variably saturated porous media: upscaling from single-pore to sample-scale model. Water Resour Res 1999;35(12):3597–606.
[87] Or D, Tuller M. Flow in unsaturated fractured porous media: Hydraulic conductivity of rough surfaces. Water Resources Res 2000;36(5):1165–77.
[88] Buckley JS, Liu Y, Monsterleet I. Mechanisms of wetting alteration by crude oils. SPE J 1998;3:54–61.
[89] Blunt MJ. Effects of heterogeneity and wetting on relative permeability using pore level modeling. SPE J 1997;2:70–87.
[90] Kovscek AR, Wong H, Radke CJ. A pore-level scenario for the development of mixed wettability in oil reservoirs. AIChE J 1993;39(6):1072–85.
[91] Dixit AB, McDougall SR, Sorbie KS. Analysis of relative permeability hysteresis trends in mixed-wet porous media using network models. In: SPE 39656, Proceedings of the SPE/DOE Improved Oil Recovery Symposium, Tulsa, OK, 19–22 April 1998.
[92] Wilkinson D, Willemsen JF. Invasion percolation: a new form of percolation theory. J Phys A 1983;16:3365–76.
[93] Toledo PG, Scriven LE and Davies HT. Pore-space statistics and capillary pressure pressure curves from volume-controlled porosimetry. In: Paper SPE 19618, Proceedings of the SPE Annual Meeting, San Antonio, TX (1989).
[94] Dullien FAL. Porous media: fluid transport and pore structure. second ed. San Diego: Academic Press; 1992.
[95] Zhou D, Blunt MJ, Orr FM. Hydrocarbon drainage along corners of noncircular capillaries. J Colloid Interf Sci 1997;187: 11–21.
[96] Goode PA, Ramakrishnan TS. Momentum transfer across fluid–fluid interfaces in porous media: a network model. AIChE J 1993;39(7):1124–34.
[97] Oak MJ. Three-phase relative permeability of water-wet berea. In: Paper SPE 20183, Proceedings of the SPE/DOE Seventh Symposium on Enhanced Oil Recovery, Tulsa, Oklahoma, 22–25 April 1990.
[98] Amott A. Observations relating to the wettability of porous rock. Trans AIME 1959;216:156–62.

[99] van Dijke MIJ, Sorbie KS, McDougall SR. Saturation-dependencies of three-phase relative permeabilities in mixed-wet and fractionally-wet system. Adv Water Resources 2001;24:365–84.
[100] Larouche C, Vizika O, Kalaydjian F. Network modeling as a tool to predict three-phase gas injection in heterogeneous wettability porous media. J Petroleum Sci Eng 1999;24:155–68.
[101] Pereira GG, Pinczewski WV, Chan DYC, Paterson L, Øren PE. Pore-scale network model for drainage dominated three-phase flow in porous media. Transport Porous Med 1996;24(2):167–201.
[102] Larsen JK, Bech N, Winter A. Three-phase immiscible WAG injection: micromodel experiments and network models. In: SPE 59324, Proceedings of the SPE/ODE Improved Oil Recovery Symposium, Tulsa, OK, 3–5 April 2000.
[103] Soll WE, Celia MA. A modified percolation approach to simulating three-fluid capillary pressure–saturation relationships. Adv Water Resources 1993;16:107–26.
[104] Heiba AA, Davis HT, Scriven LE. Statistical network theory of three-phase relative permeabilities. In: Paper SPE 12690, Proceedings of the SPE/DOE Symposium on Enhanced Oil Recovery, Tulsa, OK, 15–18 April 1984.
[105] Blunt MJ. An empirical model for three-phase relative permeability. SPE J 2000;5:435–45.
[106] Stone HL. Probability model for estimating three-phase relative permeability. J Petroleum Technol 1970;8:214–8.
[107] Baker LE. Three-phase relative permeability correlations. In: Paper SPE 17369, Proceedings of the SPE/DOE Symposium on Enhanced Oil Recovery, Tulsa, OK, 17–20 April 1988.
[108] Bartell FE, Osterhoff HJ. Determination of wettability of a solid by a liquid. Indust Eng Chem 1927;19:1277–87.
[109] Zhou D, Blunt MJ. Effect of spreading coefficient on the distribution of light non-aqueous phase liquid in the subsurface. J Contaminant Hydrology 1997;25:1–19.
[110] Blunt MJ. Constraints on contact angles for multiple phases in thermodynamic equilibrium. J Colloid Interf Sci 2001;239:281–2.
[111] DiCarlo DA, Sahni A, Blunt MJ. Effect of wettability on three-phase relative permeability. Transport Porous Med 2000;39:347–66.
[112] DiCarlo DA, Sahni A, Blunt MJ. Three-phase relative permeability of water-wet, oil-wet and mixed-wet sandpacks. SPE J 2000;5(1):82–91.
[113] Moulu JC, Vizika O, Egermann P, Kalaydjian F. A New Three-phase relative permeability model for various wettability conditions. In: Paper SPE 56477, Proceedings of the Annual Technical Conference and Exhibition of the Society of Petroleum Engineers, Houston, TX, 3–6 October 1999.
[114] Firincioglu T, Blunt MJ, Zhou D. Three-phase flow and wettability effects in triangular capillaries. Colloids Surf A 1999;155:259–76.
[115] Sahni A, Burger J, Blunt MJ. Measurement of three phase relative permeability during gravity drainage using CT scanning. In: Paper SPE 39655, Proceedings of the SPE/DOE Improved Oil Recovery Symposium, Tulsa, OK, 19–22 April 1998.
[116] Grader AS, O'Meara DJ. Dynamic displacement measurements of three-phase relative permeabilities using three immiscible liquids. In: Paper SPE 18293, Proceedings of the SPE Annual Technical Conference and Exhibition of the Society of Petroleum Engineers, Houston, TX, 2–5 October 1988.
[117] Øren PE, Billiote J, Pinczewski WV. Mobilization of waterflood residual oil by gas injection for water-wet conditions. SPE Formation Evaluation 1992;7:70–8.
[118] Keller AA, Blunt MJ, Roberts PV. Micromodel observation of the role of oil layers in three phase flow. Transport Porous Med 1997;26:277–97.
[119] van Dijke MIJ, Sorbie KS. The effects of wettability on three-phase flow in porous media: basic theory and network modelling results. SCA 2001-36, Proceedings of the 2001 International Symposium of the Society of Core Analysts, Murrayfield, Edinburgh, 17–19 September 2001.
[120] Sohrabi M, Henderson GD, Tehrani DH, Danesh A. Visualisation of oil recovery by water alternating gas (WAG) injection using high pressure micromodels—water-wet system. SPE 63000, Proceedings of the SPE Annual Technical Conference and Exhibition held in Dallas, Texas, 1–4 October 2000.
[121] Sahni A, Guzman R, Blunt MJ. Theoretical analysis of three phase flow experiments in porous media. In: Paper SPE 36664, Proceedings of the SPE Annual Technical Conference and Exhibition, Denver, CO, 6–9 October 1996.
[122] Guzman RE, Fayers FJ. Mathematical properties of three-phase flow equations. SPE J 1997;2:291–300.
[123] Guzman RE, Fayers FJ. Solutions to the three-phase Buckley–Leverett problem. SPE J 1997;2:301–11.
[124] Bora R, Maini BB, Chakma A. Flow visualization studies of solution gas drive process in heavy oil reservoirs with a glass micromodel. SPE Reservoir Evaluation Eng 2000;3:224–9.
[125] Du C, Yortsos YC. A numerical study of the critical gas saturation in a porous medium. Transport Porous Med 1999;35(2):205–25.
[126] Jamiolahmady M, Danesh A, Tehrani D, Duncan DB. A mechanistic model of gas-condensate flow in pores. Transport Porous Med 2000;41(1):17–46.
[127] Bruderer C, Bernabé Y. Network modeling of dispersion: Transition from Taylor dispersion in homogeneous networks to mechanical dispersion in very heterogeneous ones. Water Resources Res 2001;37(4):897–908.
[128] Mogensen K, Stenby E. A dynamic two-phase pore-scale model of imbibition. Transport Porous Med 1998;32(3):299–327.
[129] Payatakes AC. Dynamics of oil ganglia during immiscible displacement in water-wet porous media. Ann Rev Fluid Mech 1982;14:365–93.
[130] Aker E, Måløy KJ, Hansen A, Batrouni GG. A two-dimensional network simulator for two-phase flow in porous media. Transport Porous Med 1998;32(2):163–86.
[131] Blunt MJ, Scher H. Pore level modeling of wetting. Phys Rev E 1995;52:6387–403.
[132] Glass RJ, Nicholl MJ, Yarrington L. A modified invasion percolation model for low-capillary number immiscible displacements in horizontal rough-walled fractures: influence of local in-plane curvature. Water Resources Res 1998;34(12):3215–34.
[133] Jerauld GR. General three-phase relative permeability model for Prudhoe Bay. In: Paper SPE 36178, Proceedings of the 7th ADIPEC, Abu Dubai, 13–16 October 1996.
[134] Killough JE. Reservoir simulation with history-dependent saturation functions. SPE J 1976;16:37–48.
[135] Jackson MD, Valvatne PH, Blunt MJ. Prediction of wettability variation and its impact on flow using pore- to core- to reservoir-scale simulations. Proceedings of the International Energy Agency Meeting, Vienna, September 2001.
[136] Heiba AA, Jerauld GR, Davis HT, Scriven, LE. Mechanism-based simulation of oil recovery processes. In: Paper SPE 15593, Proceedings of the 61st SPE Annual Technical Conference, New Orleans, 5–8 October 1986.